Electroresponsive Behavior of a Sulfonated Poly(vinyl alcohol) Hydrogel and Its Application to Electrodriven Artificial Fish

Shiwen Yang, Genqi Liu, Xiaoqiang Wang, Jinyue Song

Department of Applied Chemistry, Northwestern Polytechnical University, Chang'an District, Xi'an 710129, People's Republic of China

Received 27 August 2009; accepted 7 January 2010
DOI 10.1002/app.32069

ABSTRACT: A novel sulfonated poly(vinyl alcohol) hydrogel was prepared by the sulfonation of a semicarbonized poly(vinyl alcohol) hydrogel with concentrated sulfuric acid, and its swelling properties, mechanical properties, and electroresponsive behavior in Na_2SO_4 solutions were studied. The results indicated that the hydrogel had a sandwich-type structure, and this was confirmed by scanning electron microscopy. The water take-up ability of the hydrogel decreased with the ionic strength of the Na_2SO_4 solution increasing. Young's modulus, the elongation at break, and the tensile strength of the hydrogel swollen in deionized water were 1.36 MPa, 165%, and 2.93 MPa, respectively. The hydrogel swollen in an Na_2SO_4 solution bent toward the cathode under noncontact direct-current electric fields, and its bending speed and equilibrium strain increased with the applied voltage increasing. There was a critical ionic strength of 0.03 at which the maximum equilibrium strain of the hydrogel occurred. With cyclical changes in the direction of the applied potential, the hydrogel exhibited good reversible bending behavior. On this basis, an artificial fish was designed. Under a cyclically varying electric field (the period was 2 s, and the voltage ranged from −15 to 15 V), the swimming speed of the artificial fish could reach 9.6 cm/min in an Na_2SO_4 solution with an ionic strength of 0.03. © 2010 Wiley Periodicals, Inc. J Appl Polym Sci 117: 2346–2353, 2010

Key words: crosslinking; hydrogels; stimuli-sensitive polymers

INTRODUCTION

A polymer hydrogel is a kind of material with a three-dimensional, hydrophilic, polymeric network capable of imbibing large amounts of water. In recent years, polymer hydrogels have attracted much attention as intelligent materials because of their special characteristics.[1–5] They can change their volume and shape reversibly in response to external stimuli, such as changes in the pH,[6–8] solvent composition,[9,10] temperature,[11–13] light,[14] and electric field.[15,16] Among the various kinds of intelligent hydrogels, electric-field-responsive hydrogels seem to be particularly interesting because an electric field is the most conventional and convenient stimulus with respect to signal control. Therefore, the study of electroresponsive hydrogels has become very hot in recent years.[17–22] Electric-field-induced bending deformation or volume changes in polyelectrolyte hydrogels can transform chemical free energy directly into mechanical work to yield isothermal energy conversion, and they can be used as actuators, electromechanical engines, artificial muscles,[23–25] chemical values,[26] and controlled drug delivery devices.[27–29]

However, to realize a powerful actuator or a material close to skeletal muscles, polymer gels with both fast and sensitive electric responses and a high degree of mechanical strength are necessary. Poly(vinyl alcohol) (PVA) is a water-soluble polyhydroxyl polymer employed in practical applications because of its easy preparation, excellent chemical resistance and physical properties, and complete biodegradability. Therefore, some researchers have prepared interpenetrating polymer network or semi-interpenetrating polymer network electroresponsive hydrogels with PVA as a matrix material because of its excellent mechanical properties.[29–32] However, because PVA hydrogels are nonelectrolyte hydrogels and do not respond to an electric field, with increasing

---

Correspondence to: G. Liu (liugenqi@nwpu.edu.cn).

Contract grant sponsor: Northwestern Polytechnical University Foundation for Fundamental Research; contract grant number: NPU-FFR-JC200823.

Contract grant sponsor: Developing Program for Outstanding Persons in Northwestern Polytechnical University; contract grant number: 521020101-1101-03XD0106.

Journal of Applied Polymer Science, Vol. 117, 2346–2353 (2010)

mechanical properties, the electroresponsive speed and intensity of the hydrogels can be weakened at the same time.

Electrodriven chemomechanics based on intelligent hydrogels is a rising-front field. Osada et al.[15] reported a gel looper made of a poly(2-acrylamido-2-methyl propane) sulfonic acid (PAMPS) hydrogel with a maximum crawling velocity of 25 cm/min in a 0.03 mol/L Na_2SO_4 and 0.01 mol/L *n*-dodecyl pyridinium chloride ($C_{12}PyCl$) mixed solution at the electric field strength of 10 V/cm. Kim et al.[33] reported a soft, fishlike machine with a tail also made of a PAMPS hydrogel that could achieve the swimming speed of 15 cm/min in a 0.03 mol/L Na_2SO_4 and 0.01 mol/L $C_{12}PyCl$ mixed solution at the electric field strength of 1.4 V/cm. The purpose of using surfactants is to enhance the stimulus response speed and mechanical properties of PAMPS hydrogels. However, surfactants are environmental pollutants, and it is inconvenient and unrealistic to add a surfactant to an electrolyte in practical applications of these moving systems.

In this study, a novel electroresponsive sulfonated poly(vinyl alcohol) (S-PVA) hydrogel with a sandwich-type structure and a high mechanical strength was prepared by semicarbonization of a PVA hydrogel film and then sulfonation with concentrated sulfuric acid. Its swelling properties, mechanical properties, and electroresponsive behavior in Na_2SO_4 solutions were studied. Meanwhile, because of the electroresponsive performance of the S-PVA hydrogel, a new type of artificial fish was designed with the S-PVA hydrogel used for its tail fin. Under a cyclically varying electric field (the period was 2 s, and the voltage ranged from −15 V to 15 V), the artificial fish showed fishlike motion, and its swimming speed could reach 9.6 cm/min in an Na_2SO_4 solution with an ionic strength of 0.03. It has potential applications in the fields of pipeline inspection, marine exploration, and so forth.

EXPERIMENTAL

Materials

PVA (polymerization degree = 1700 ± 50, saponification = 99.9%) was purchased from Beibei Chemicals Manufacturer (Chongqing, China). An aqueous glutaraldehyde (GA) solution (25%) was purchased from China Medicine (Group) Shanghai Chemical Reagent Corp. (Shanghai, China). Concentrated sulfuric acid (98%, analytical grade) was supplied by Shantou Xilong Chemical Factory (Guangdong, China), and sodium sulfate (analytical grade) was purchased from Tianjin Chemical Reagent Factory (Tianjin, China). All reagents were used without further purification.

Preparation of the chemically crosslinked PVA hydrogels

PVA (0.89 g) was dissolved in deionized water to form a 5.0 wt % solution at 90°C. After it cooled to 50°C, 0.5 mL of 1 mol/L HCl and 0.89 mL of a 1.0 wt % GA solution were added to the solution with vigorous stirring for 1 min. Then, the resultant solution was poured into a Plexiglas tank (10 mm × 6 mm × 2 mm) and heated at 50°C until a dry film of the PVA hydrogel formed. Then, the film was taken out and immersed in deionized water for 3 days to remove the unreacted chemicals, and it was dried in a 40°C vacuum oven for 2 days.

Semicarbonization of the PVA hydrogel

For semicarbonization, the dried PVA hydrogel film was put into an oven at 180°C and heated for 1 h. The transparent PVA hydrogel film turned light yellow after semicarbonization. The semicarbonized PVA hydrogel was very rigid and did not swell in water.

Preparation of the S-PVA hydrogel

The semicarbonized PVA hydrogel film was cut into 3 cm × 3 cm pieces and then immersed in concentrated sulfuric acid for 2 min. The resultant hydrogel was washed with 20 wt % H_2SO_4 at first and then washed with deionized water until the washing liquid was neutral; finally, it was immersed in deionized water for 4 days to remove the soluble substances. During that time, the water was changed once every 8 h, and then the hydrogel was dried in a vacuum oven at 40°C until a constant weight was obtained.

IR analysis

IR spectra of the pure PVA, PVA hydrogel, semicarbonized PVA hydrogel, and S-PVA hydrogel samples were recorded on a Tensor 27 IR spectrometer (Bruker Corp., Ettlingen, Germany) with a KBr pellet technique.

Scanning electron microscopy (SEM) analysis

An SEM micrograph of the freeze-dried gel was obtained to visualize the cross section of the S-PVA hydrogel. A small section of the S-PVA hydrogel was cut from a swollen gel sheet with a sharp blade, blotted on filter paper for removal of the excess surface water, and then lyophilized with a freeze-drier (model Alpha 1-2/LD, Martin Christ, Osterode, Germany) for 12 h. After freeze drying, the cross section of the specimen was sputter-deposited with gold before SEM observation. The microstructure of the

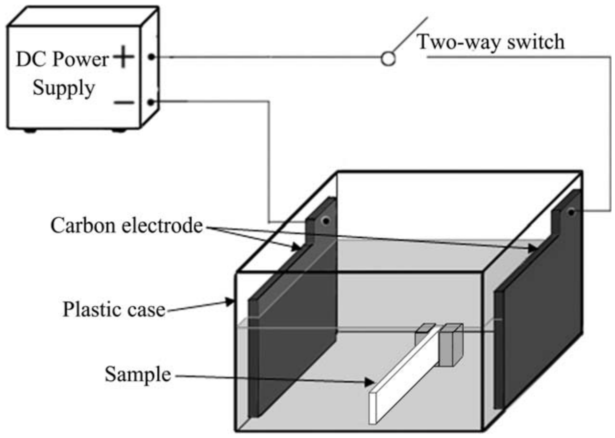

Figure 1 Self-made equipment for measurement under a dc electric field.

freeze-dried hydrogel was imaged with a field-emission scanning electron microscope (Supra 55, Zeiss, Germany) operated at an excitation voltage of 12 kV.

Swelling properties of the S-PVA hydrogel

To measure the swelling ratio (S_w), preweighed dry samples of the hydrogels were immersed in aqueous Na_2SO_4 solutions. After the removal of the excess surface water with filter paper, the weights of the hydrogel samples were measured at various time intervals. S_w was determined according to the following equation:

$$S_w = \frac{W_t - W_d}{W_d} \tag{1}$$

where W_t and W_d are the weights of a sample at time t and in the dry state, respectively.

Mechanical strength properties of the S-PVA hydrogel

The tensile strength, elongation at break, and Young's modulus of the S-PVA hydrogel were measured by the static stretching method. The S-PVA sample was fully swollen in deionized water and cut into 30 mm × 3 mm × 0.16 mm strips for use.

Electroresponsive behavior of the S-PVA hydrogel under a direct-current (dc) electric field

An aqueous Na_2SO_4 solution was poured into a plastic case equipped with two parallel carbon electrodes (Fig. 1). The distance between them was 30 mm. The S-PVA hydrogel was fully swollen in the aqueous Na_2SO_4 solution at room temperature, and it was cut into 10 mm × 3 mm × 0.16 mm strips. One end of the sample was fixed, and the hydrogel was placed in the center of the case. The electroresponsive behavior of the hydrogel was investigated by the measurement of the displacement of its free end, that is, the deflection of bending (Y) before and after the electric field was applied. The sign of the deflection was considered positive when the hydrogel bent to the cathode. The strain of bending (ε) was calculated with the following equation:[24]

$$\varepsilon = \frac{6DY}{L^2} \tag{2}$$

where Y is the deflection of bending, D is the thickness of the hydrogel, and L is the original length of the hydrogel before the application of the electric field. To test the reversible bending behavior of the hydrogel strips, we altered the polarity of the electric field every 20 s by changing a two-way switch.

RESULTS AND DISCUSSION

IR analysis

In the IR spectrum of pure PVA [Fig. 2(a)], the absorption bands at 3342 and 2941 cm^{-1} are the stretching vibrations of —OH and C—H, respectively. In comparison with the IR spectrum of PVA, the absorbance of the absorption band at 1094 cm^{-1} (the stretching vibration of C—O—C) in the IR spectrum of the PVA hydrogel [Fig. 2(b)] is increased, and this indicates that PVA crosslinked with GA successfully.[34] A comparison of the IR spectra of the PVA hydrogel and semicarbonized PVA shows that no new absorption peak was generated, but the ratio of the relative absorption intensities at 1094 (the stretching vibration of C—O—C) and 3386 cm^{-1} (the stretching vibration of —OH) increased after the semicarbonization treatment of the PVA hydrogel

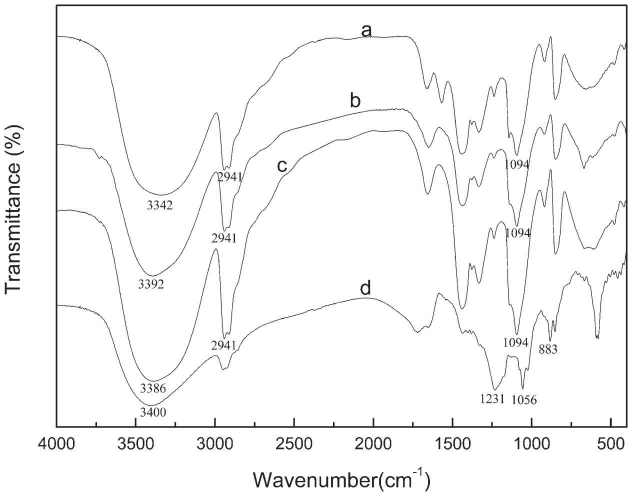

Figure 2 IR spectra of (a) pure PVA, (b) PVA hydrogel, (c) semicarbonized PVA hydrogel, and (d) S-PVA hydrogel.

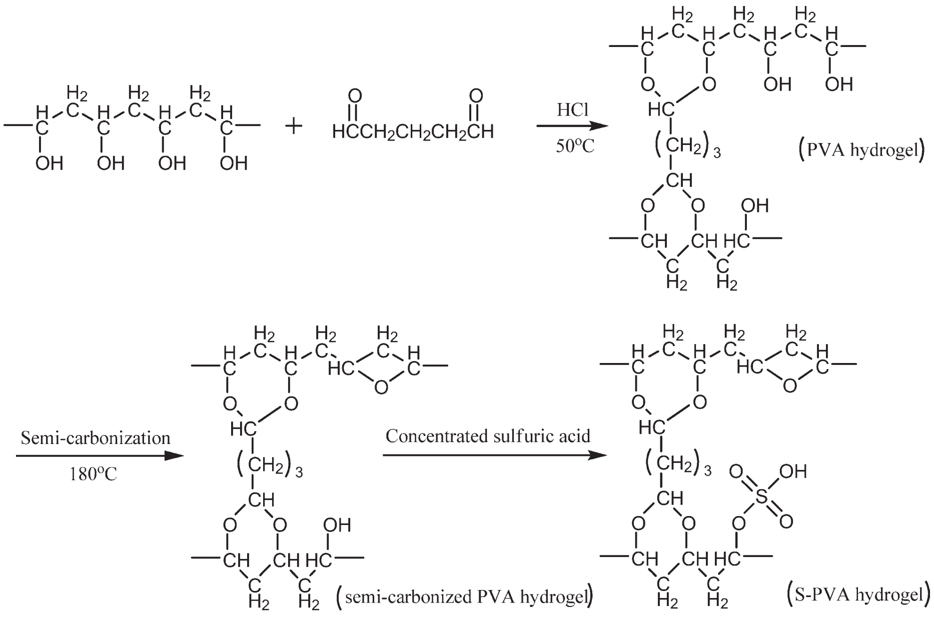

Scheme 1 Chemical reaction flow chart for the preparation of the S-PVA hydrogel.

[Fig. 2(c)], and this indicates that the content of C—O—C groups increased, whereas the content of —OH groups decreased at the same time. This occurred because the purpose of semicarbonization is to reduce the content of hydroxyl in the PVA hydrogel and to enhance its mechanical strength and oxidation resistance.[35] Meanwhile, absorption bands at 1231 (the S=O stretching vibration of —SO_3H) and 883 cm^{-1} (the S—O stretching vibration of —SO_3H)[36] appear in the IR spectrum of the S-PVA hydrogel [Fig. 2(d)]. The drastic changes in the spectrum of S-PVA indicate effective sulfonation of the semicarbonized PVA hydrogel. The chemical reaction flow chart for the preparation of the S-PVA hydrogel is shown in Scheme 1.

SEM analysis

Figure 3 shows the microstructures of the cross section of the S-PVA hydrogel. The S-PVA hydrogel has a sandwich-type structure. Meanwhile, the middle part of the S-PVA hydrogel is quite compact, but both sides are quite loose. This phenomenon is due to the fact that the semicarbonized PVA hydrogel does not swell in concentrated sulfuric acid, so the sulfonation reaction occurs at the surface layers first, and the middle of the PVA hydrogel is unsulfonated or less sulfonated.

Swelling properties of the S-PVA hydrogel

Figure 4 shows the swelling kinetic curves of the S-PVA hydrogel in aqueous Na_2SO_4 solutions of different ionic strengths. S_w decreased with the ionic strength of the Na_2SO_4 solution increasing. This can be explained as follows: with the ionic strength of the Na_2SO_4 solution increasing, a shielding effect caused by the counterions in the electrolytic solution occurred, and this led to a reduction in the electrostatic repulsion of the polyions and a decrease in S_w of the hydrogel.

Mechanical properties of the S-PVA hydrogel

The experimentally measured elongation at break and tensile strength of the hydrogel are 165% and 2.93 MPa, respectively. Figure 5 shows the stress–strain curve of the S-PVA hydrogel swollen in deionized water. The curve indicates that Young's modulus of the hydrogel is 1.36 MPa. Meanwhile, the mechanical properties were compared with a

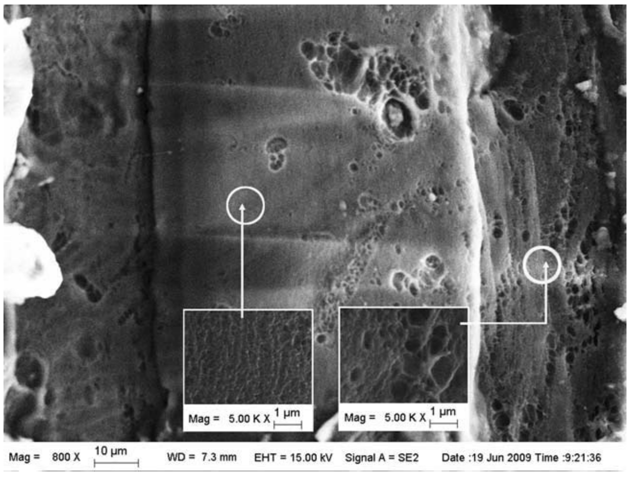

Figure 3 Microstructure of the cross section of the S-PVA hydrogel.

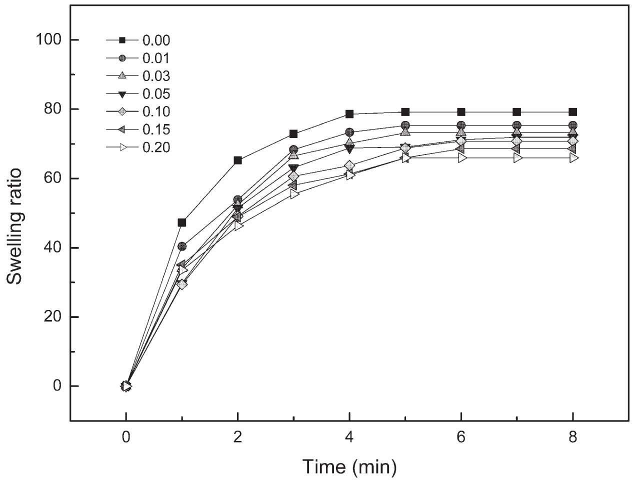

Figure 4 Swelling kinetic curves of S-PVA hydrogels with aqueous Na_2SO_4 solutions of different ionic strengths.

gelatin hydrogel,[37] a chitosan hydrogel,[38] and a semi-IPN PNIPAm/PAM hydrogel,[39] as shown in Table I. The results indicate that the mechanical properties of the S-PVA hydrogel are very good. The tensile strength, Young's modulus, and ultimate stress of rat skeletal muscle have been reported to be 0.5 ± 0.05 MPa, 0.43 ± 0.083 MPa, and 88.0 ± 7.84%, respectively.[40] Thus, the mechanical properties of the S-PVA hydrogel greatly exceed those of natural muscles, so the S-PVA hydrogel may be used as a powerful actuator or artificial muscle in practice.

Electroresponsive behavior of the S-PVA hydrogel under an electric field

When an S-PVA hydrogel strip swollen in an aqueous Na_2SO_4 solution was subjected to a dc electric field, it bent toward the cathode. When the polarity of the electric field was changed, the hydrogel strip first became straight and then bent in the opposite direction.

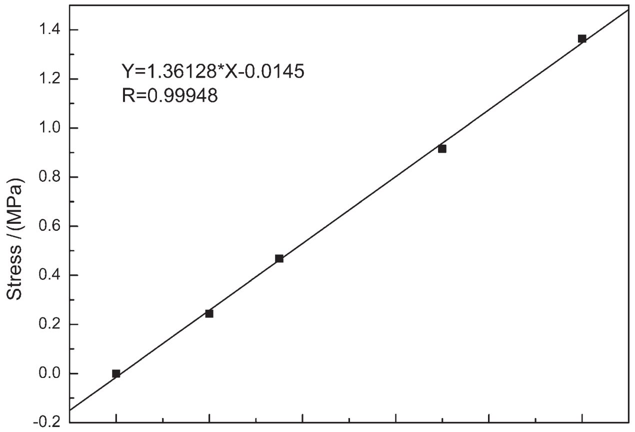

Figure 5 Stress–strain curve of the S-PVA hydrogel swollen in deionized water (R: linear correlation coefficient).

TABLE I
Mechanical Properties of Several Electroresponsive Hydrogels

	Hydrogel			
	S-PVA in deionized water	Gelatin in 0.01 mol/L NaCl	Chitosan in deionized water	Semi-IPN PNIPAm/PAM in deionized water
E (MPa)	1.36	4.29×10^{-3}	–	0.101
P_t (MPa)	2.93	5.11×10^{-3}	3.43×10^{-3}	–
ε_t (%)	165	110	58.0	–

ε_t = elongation at break; E = Young's modulus; P_t = tensile strength.

The sulfonic acid group is a strong anionic electrolyte group, so the hydrogel is a polyanionic hydrogel. When an electric field is applied to the negatively charged hydrogel in an aqueous solution, the counterion of the polyion moves toward the negative electrode, whereas the polyion remains immobile. Also, the free ions in the surrounding solution move toward their counter electrodes and come into the hydrogel. Thus, the osmotic pressure on the anode side becomes larger than that on the cathode side, and the gel bends toward the cathode. Consequently, the osmotic pressure difference occurs within the hydrogel, and it is the driving force of the bending toward the negative electrode.

The electroresponsive behavior of the hydrogel was affected by the ionic strength of the aqueous Na_2SO_4 solution. Figure 6 shows the correlation between the equilibrium strain and ionic strength of the aqueous Na_2SO_4 solution at different voltages at

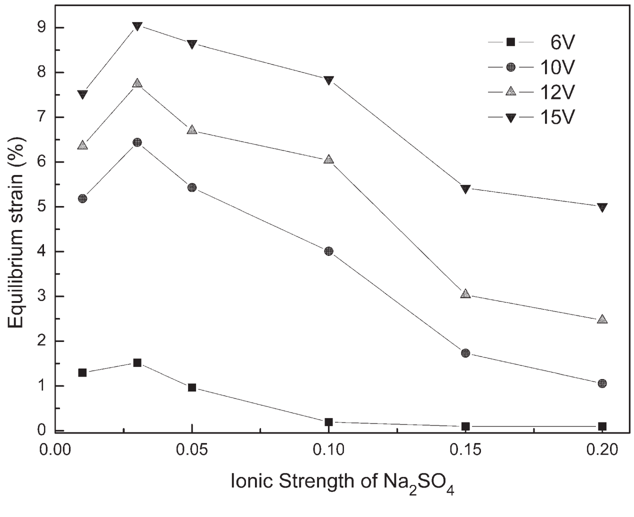

Figure 6 Effect of the ionic strength of the aqueous Na_2SO_4 solution on the equilibrium strain under different applied voltages: 6, 10, 12, and 15 V.

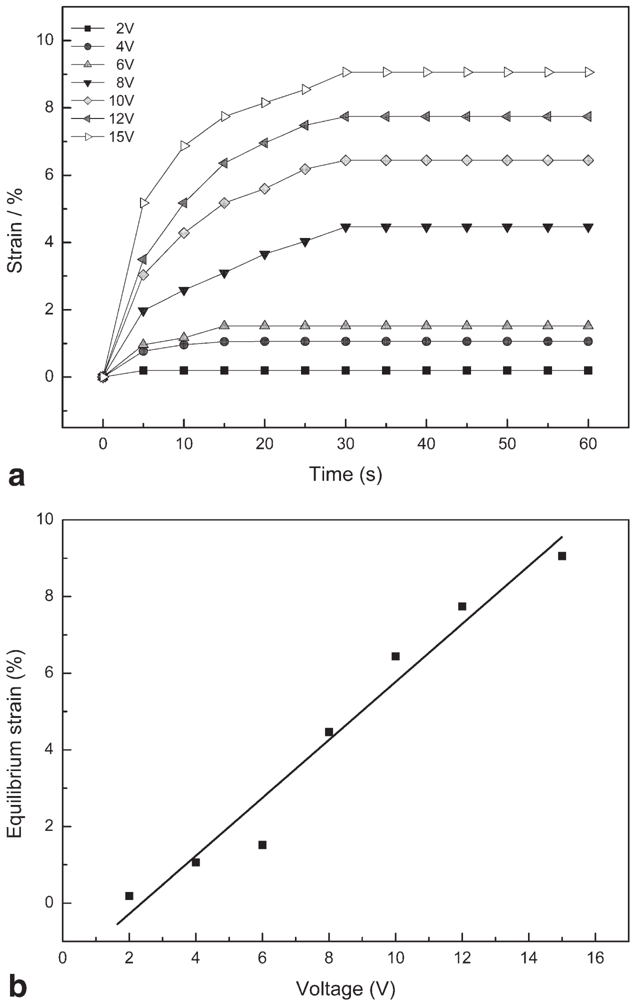

Figure 7 (a) Bending kinetic curves and (b) equilibrium strain of S-PVA hydrogels under different applied voltages in an $I = 0.03$ Na_2SO_4 solution.

room temperature. With the ionic strength of the aqueous Na_2SO_4 solution increasing, the equilibrium strain increased first and then decreased gradually. The maximum equilibrium strain occurred when the ionic strength of the aqueous Na_2SO_4 solution was 0.03. As described previously, an increase in the electrolyte concentration of a solution induces an increase in the number of free ions moving from the surrounding solution toward their counter electrodes and into the hydrogel itself. As a result, the strain of the hydrogel increases. However, if the ionic strength of the Na_2SO_4 solution is greater than the critical ionic strength of 0.03, a shielding effect of the polyions caused by the counterions in the electrolytic solution will occur, and this will lead to a reduction in the electrostatic repulsion of the polyions and a decrease in the equilibrium strain.

Figure 7 shows the bending kinetic curves and equilibrium strain of the S-PVA hydrogel at different applied voltages in an aqueous Na_2SO_4 solution with an ionic strength of 0.03. As shown in Figure 7(a), the gradient slope in the plot of ε versus time becomes steeper with the applied voltage increasing and then levels off in a steady state. The bending speed and equilibrium strain increase with the applied voltage increasing, and this can be explained by the fact that there is an enhancement in the transfer rate of the counterions of the immobile $—SO_3^-$ groups on the hydrogel network from the hydrogel to the external solution, and the free ions move from the external solution into the hydrogel as the potential gradient in the electric field is increased. A further analysis of the relationship between the voltage amplitude and the equilibrium strain shows a linear correlation between them [Fig. 7(b)]. These quantitative relationships could be useful in the design of actuator devices.

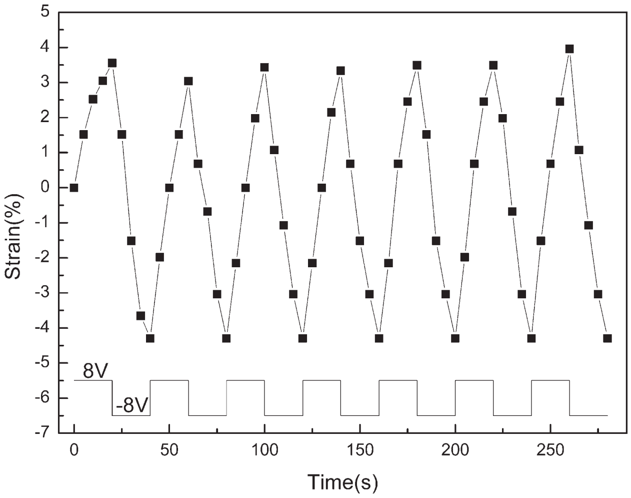

Figure 8 Response of bending for S-PVA hydrogels under an electric field cyclically varying from 8 to −8 V every 20 s ($I = 0.03$).

In addition, the reversible bending behavior of the hydrogel, depending on an electric stimulus, was examined. When an electric field was applied to a strip of the hydrogel, it bent toward the negative electrode. When the electric stimulus was removed, the gel was gradually displaced to its original

Figure 9 View of the developed artificial fish.

position. Also, if the polarity of the electric field was altered, the hydrogel bent in the opposite direction. When a cyclic electric field was applied, with the reversal of the electric field direction, the hydrogel bent quickly in the opposite direction without hysteresis. Figure 8 indicates that the S-PVA hydrogel exhibited good reversible bending behavior under an electric field cyclically varying from 8 to −8 V every 20 s.

Design of an electrodriven artificial fish with the S-PVA hydrogel

On the basis of the electroresponsive performance of the S-PVA hydrogel, a new type of artificial fish was designed. The artificial fish was made with silicone rubber, a small wood clip, and a piece of the S-PVA hydrogel film. The prototype of the developed artificial fish is shown in Figure 9. The specifications of the artificial fish are shown in Table II.

The body was made of silicone rubber, which provided buoyancy for the hydrogel fish. The small wood clip was used to link the body and the S-PVA hydrogel film. A pair of parallel carbon electrodes were placed 30 mm apart in an Na_2SO_4 solution (I = 0.03), and a potential of 15 V was applied. The fish swam forward by repeated swinging of the S-PVA hydrogel tail. Figure 10 shows photographs of the swimming artificial fish at different times. The speed of the gel fish was about 9.6 cm/min under the experimental conditions.

Our moving system, because no surfactant is used, will be very convenient to use and has potential applications in the fields of pipeline inspection, marine exploration, and so forth. However, our artificial fish, because of its lack of balance, showed extensive swinging of the head as a result of counterbalancing of the motion of the tail, and this might have decreased the efficiency of the forward motion; therefore, further improvement of the design will be required.

CONCLUSIONS

A novel S-PVA hydrogel with a sandwich-type structure was prepared by sulfonation of a semicarbonized PVA hydrogel with concentrated sulfuric acid. The water take-up ability of the hydrogel increased with the ionic strength of the aqueous Na_2SO_4 solution decreasing. Under a noncontact dc electric field, the hydrogel strip showed electroresponsive behavior. The bending behavior could be adjusted via the voltage of the applied electric field and the ionic strength of the electrolyte. With repeated changes in the direction of the applied potential, the hydrogel strip exhibited good reversible bending behavior. An artificial fish based on the S-PVA hydrogel was designed and had a swimming speed of 9.6 cm/min in an Na_2SO_4 solution with an ionic strength of 0.03. The hydrogel may have potential applications in high-tech fields, such as electrodriven chemomechanics, artificial muscles, and actuators.

TABLE II
Specifications of the Prototype Artificial Fish

Component	Specification
Size	52×5 mm^2
Weight	0.7635 g
Material	Body: Silicone rubber and wood clip Tail fin: S-PVA hydrogel ($15 \times 3 \times 0.16$ mm^3)

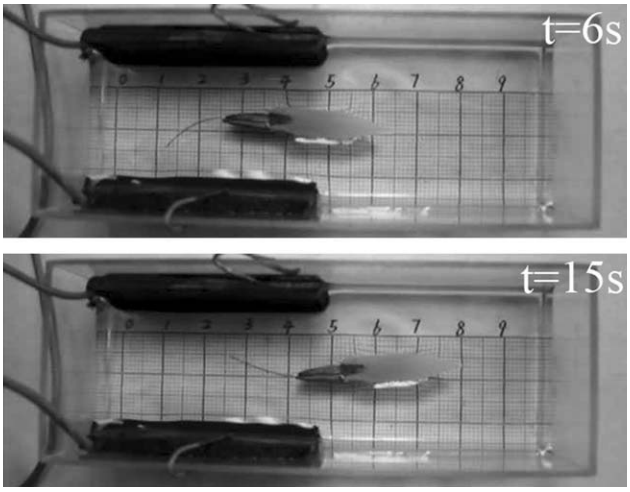

Figure 10 Progressive changes in motions of the artificial fish (electrode distance = 30 mm, voltage = 15 V).

References

1. Dong, L.; Agarwal, A. K.; Beebe, D. J.; Jiang, H. R. Nature 2006, 442, 551.
2. Mahdavinia, G. R.; Zohuriaan-Mehr, M. J.; Pourjavadi, A. Polym Adv Technol 2004, 15, 173.
3. Dispenza, C.; Leone, M.; Presti, C. L.; Librizzi, F.; Vetri, V.; Spadaro, G. Macromol Symp 2007, 247, 303.
4. Richter, A.; Kuckling, D.; Howitz, S.; Gehring, T.; Arndt, K. F. J Microelectromech Syst 2003, 12, 748.
5. Zrínyi, M.; Szilágyi, A.; Filipcsei, G.; Fehér, J.; Szalma, J.; MÓczár, G. Polym Adv Technol 2001, 12, 501.
6. Chen, S. C.; Wu, Y. C.; Mi, F. L.; Lin, Y. H.; Yu, L. C.; Sung, H. W. J Controlled Release 2004, 96, 285.
7. Zhang, R. S.; Tang, M. G.; Bowyer, A.; Eisenthal, R.; Hubble, J. Biomaterials 2005, 26, 4677.
8. George, M.; Abraham, T. E. Int J Pharm 2007, 335, 123.
9. Ozmen, M. M.; Okay, O. React Funct Polym 2008, 68, 1467.
10. Pagonis, K.; Bokias, G. Polym Bull 2007, 58, 289.
11. Xu, X. D.; Zhang, X. Z.; Cheng, S. X.; Zhuo, R. X. Colloid Polym Sci 2006, 285, 75.
12. Yamamoto, H.; Heyamoto, N.; Matsui, T.; Murayama, N.; Shibata, J. Int J Thermophys 2003, 24, 1385.
13. Strachotová, B.; Strachota, A.; Uchman, M.; Šlouf, M.; Brus, J.; Pleštil, J.; Matějka, L. Polymer 2007, 48, 1471.
14. Zeng, X. F.; Jiang, H. R. Appl Phys Lett 2008, 93, 151101.

15. Osada, Y.; Okuzaki, H.; Hori, H. Nature 1992, 355, 242.
16. Shiga, T. Adv Polym Sci 1997, 134, 131.
17. Jabbari, E.; Tavakoli, J.; Sarvestani, A. S. Smart Mater Struct 2007, 16, 1614.
18. Kaewpirom, S.; Boonsang, S. Eur Polym J 2006, 42, 1609.
19. Li, H.; Luo, R.; Lam, K. Y. J Biomech 2007, 40, 1091.
20. Yoon, S. G.; Kim, I. Y.; Kim, S. I.; Kim, S. J. Polym Int 2005, 54, 1169.
21. Shang, J.; Shao, Z. Z.; Chen, X. Biomacromolecules 2008, 9, 1208.
22. Juntanon, K.; Niamlang, S.; Rujiravanit, R.; Sirivat, A. Int J Pharm 2008, 356, 1.
23. Schreyer, H. B.; Gebhart, N.; Kim, K. J.; Shahinpoor, M. Biomacromolecules 2000, 1, 642.
24. Shiga, T.; Hirose, Y.; Okada, A.; Kurauchi, T. J Appl Polym Sci 1992, 44, 249.
25. Kudaibergenov, S. E.; Sigitov, V. B. Langmuir 1999, 15, 4230.
26. Osada, Y.; Ross-Murphy, S. B. Sci Am 1993, 268, 482.
27. Kagatani, S.; Shinoda, T.; Konno, Y.; Fukui, M.; Ohmura, T.; Osada, Y. J Pharm Sci 1997, 11, 1273.
28. Kwon, I. C.; Bae, Y. H.; Kim, S. W. Nature 1991, 354, 291.
29. Kim, S. Y.; Lee, Y. M. J Appl Polym Sci 1999, 74, 1752.
30. Lin, S. B.; Yuan, C. H.; Ke, A. R.; Quan, Z. L. Sens Actuators, B 2008, 134, 281.
31. Kim, S. J.; Yoon, S. G.; Lee, Y. M.; Kim, S. I. Sens Actuators B 2003, 88, 286.
32. Kim, S. J.; Yoon, S. G.; Lee, S. M.; Lee, S. H.; Kim, S. I. J Appl Polym Sci 2004, 91, 3613.
33. Kim, B. S.; Gong, J. P.; Osada, Y. Polym Int 1999, 48, 691.
34. Choong-Kyun, Y.; Kew-Ho, L. J Membr Sci 1996, 109, 257.
35. Lu, Y.; Zhang, H. J Tianjin Polytechnic Univ 2004, 6, 5.
36. Gao, H. H.; Shi, G. Q.; Wang, Y.; Wu, G. F.; Chen, H. S. China Pulp Pap 2005, 24, 29.
37. Liu, G. Q.; Zhao, X. P. J Macromol Sci Pure Appl Chem 2005, 42, 51.
38. Yin, Y. J.; Yao, K. D.; Cheng, G. X.; Ma, J. B. Polym Int 1999, 48, 429.
39. Muniz, E. C.; Geuskens, G. J Mater Sci Mater Med 2001, 12, 879.
40. Zhang, S. N.; Lu, S. Y. Chin J Sports Med 2005, 24, 261.